

1 **Gene-level, but not chromosome-wide, divergence between a very young**  
2 **house fly Y chromosome and its homologous X chromosome**

3

4 Jae Hak Son<sup>1,2,3</sup> and Richard P. Meisel<sup>1,4</sup>

5

6 1. Department of Biology and Biochemistry, University of Houston, Houston, TX, USA

7

8 2. Current Address: Department of Epidemiology of Microbial Diseases, Yale School of Public  
9 Health, New Haven, CT, USA

10

11 3. Jae Hak Son: [jaehak.son@yale.edu](mailto:jaehak.son@yale.edu)

12

13 4. Richard P. Meisel: [rpmeisel@uh.edu](mailto:rpmeisel@uh.edu)

14 **Abstract**

15

16 X and Y chromosomes are derived from a pair of homologous autosomes, which then diverge  
17 from each other over time. Although Y-specific features have been characterized in sex  
18 chromosomes of various ages, the earliest stages of Y chromosome evolution are poorly  
19 understood. In particular, we do not know whether early stages of Y chromosome evolution  
20 consist of changes to individual genes or happen via chromosome-scale divergence from the X.  
21 To address this question, we used house fly, *Musca domestica*, as a model because it has very  
22 young sex chromosomes that are still segregating as polymorphisms within natural populations.  
23 To identify early differentiation between the very young X and Y chromosomes, we compared  
24 genotypic (XY) and sex-reversed (XX) males in gene sequence and gene expression using RNA-  
25 seq and Oxford Nanopore sequencing data. There is an excess of genes with divergent  
26 expression between the X and Y copies, but the number of genes is small. This suggests that  
27 individual Y genes, but not the entire Y chromosome, have diverged from their homologous X-  
28 linked alleles. We identified one gene, encoding an axonemal dynein assembly factor (which  
29 functions in sperm motility), that has higher expression in the abdomens of XY males than XX  
30 males because of a disproportionate contribution of the Y allele to gene expression. The up-  
31 regulation of the Y-linked copy of this gene may be favored in males because of its function in  
32 spermatogenesis, consistent with sexually antagonistic selection affecting the expression  
33 evolution of individual genes during early Y chromosome evolution.

## 34 Introduction

35

36 In many organisms with two separate sexes, a gene on a sex chromosome determines whether an  
37 individual develops into a male or female. In XX/XY sex chromosome systems, males are the  
38 heterogametic sex (XY genotype), and females are homogametic with the XX genotype (Bull  
39 1983). All X and Y chromosomes are ultimately derived from a pair of ancestral autosomes that  
40 became sex chromosomes when one homolog obtained a sex-determining locus, such as a male-  
41 determining gene on a Y chromosome. The X and Y chromosomes then diverge from each other  
42 over time (Bull 1983; Charlesworth et al. 2005). Sex chromosomes have originated and diverged  
43 from each other in multiple independent evolutionary lineages (Bachtrog et al. 2014; Beukeboom  
44 and Perrin 2014)

45

46 Despite their independent origins, non-homologous Y chromosomes share many common  
47 features across species (Charlesworth et al. 2005). First, “masculinization” occurs because male-  
48 limited inheritance of the Y chromosome favors the fixation of male-beneficial genetic variants  
49 (Rice 1996). Second, suppressed recombination between the X and Y chromosomes evolves,  
50 possibly because selection favors co-inheritance of the male-beneficial alleles and the male-  
51 determining locus (Charlesworth 2018). Third, “degeneration” occurs in nonrecombining  
52 regions; functional genes that were present on ancestral autosomes become pseudogenes on the  
53 Y chromosome because suppressed recombination between the X and Y inhibits the purging of  
54 deleterious mutations in Y-linked genes (Muller’s ratchet) and enhances the effects of  
55 hitchhiking (Charlesworth and Charlesworth 2000; Bachtrog 2013; Vicoso 2019). Other  
56 common features of Y chromosomes are repetitive sequences and enlarged heterochromatic  
57 regions due to reduced effectiveness of purifying selection caused by suppressed recombination  
58 and a small effective population size (Skaletsky et al. 2003). In some cases, a mechanism evolves  
59 to compensate for the haploid dosage of X-linked genes in males, but this is not always the case  
60 (Mank 2013; Gu and Walters 2017).

61

62 Many features of Y chromosomes are thought to emerge shortly after an autosome becomes Y-  
63 linked. For example, recombination suppression has been considered to come after the  
64 emergence of a new sex-determining locus on a Y chromosome to favor the co-inheritance of the  
65 sex-determining locus and male-beneficial/female-detrimental sexually antagonistic alleles  
66 (Orzack et al. 1980; van Doorn and Kirkpatrick 2007; Roberts et al. 2009; van Doorn and  
67 Kirkpatrick 2010). As additional sexually antagonistic alleles accumulate on a Y chromosome,  
68 this is predicted to trigger progressive spread of the nonrecombining region along the Y  
69 chromosome (Rice 1987; van Doorn and Kirkpatrick 2007). Although these features have been  
70 characterized in sex chromosomes of various ages and degeneration levels (Bachtrog 2013; Zhou  
71 et al. 2014), the very first stages of Y chromosome evolution are poorly understood because of a  
72 lack of extremely young sex chromosome systems. Most of the best studied young sex  
73 chromosomes have accumulated multiple types of X-Y differentiation, including suppressed  
74 recombination, Y chromosome gene loss, or X chromosome dosage compensation (Bergero et al.  
75 2013; Mahajan et al. 2018; Darolti et al. 2019; Krasovec et al. 2019). It is therefore unclear the  
76 extent to which the early evolution of sex chromosomes is dominated by chromosome-wide X-Y  
77 divergence or gene-level differences (Kaiser et al. 2011; Zhou and Bachtrog 2012). This study  
78 addresses that shortcoming by determining how a young “proto-Y” chromosome has  
79 differentiated from its homologous proto-X chromosome shortly after its emergence.

80

81 We are especially interested in how gene expression differences accumulate between the proto-Y  
82 and proto-X chromosomes. As the proto-Y and proto-X chromosomes diverge, it is expected that  
83 alleles on the proto-Y chromosome are up- or down-regulated because of *cis*-regulatory sequence  
84 differences that contribute to proto-Y gene expression. These *cis*-regulatory effects may be  
85 especially important for the expression of sexually antagonistic (male-beneficial/female-  
86 deleterious) alleles and degeneration of functional genes (Rice 1984; Zhou and Bachtrog 2012).  
87 How these gene expression differences accumulate during the very earliest stages of sex  
88 chromosome evolution is not well understood.

89

90 We used the house fly, *Musca domestica*, as a model system to study the early evolution of sex  
91 chromosomes because it has very young sex chromosomes that are still segregating as  
92 polymorphisms within natural populations (Hamm et al. 2015). The *Musca domestica* male  
93 *determiner* (*Mdmd*) can be found on the Y chromosome ( $Y^M$ ) and on at least four autosomes  
94 (Sharma et al. 2017). Each chromosome carrying *Mdmd*, including  $Y^M$ , is a recently derived  
95 proto-Y chromosome (Meisel et al. 2017). The proto-Y and proto-X chromosomes show minimal  
96 sequence and morphological divergence, as well as similar gene content (Boyes et al. 1964;  
97 Hediger et al. 1998; Meisel et al. 2017), consistent with their recent origins. However, it is not  
98 clear the extent to which the proto-Y chromosomes are masculinized or degenerated. A previous  
99 study revealed a small, but significant, effect of the proto-Y chromosomes on gene expression  
100 (Son et al. 2019). However, it could not resolve if the expression differences are the result of  
101 changes in the expression of the proto-Y copies, proto-X copies, or both.

102

103 In this study, we tested if one proto-Y chromosome, the third chromosome carrying *Mdmd* ( $III^M$ ),  
104 has evidence of differentiation from its homologous proto-X chromosome by evaluating gene  
105 expression and DNA sequence differences between proto-Y genes and their proto-X  
106 counterparts. We compared normal (genotypic) males carrying a  $III^M$  proto-Y chromosome to  
107 sex-reversed males with no proto-Y chromosome using RNA-seq data generated in a previous  
108 study (Son et al. 2019) and newly generated Nanopore long read sequencing data. The genotypic  
109 males contain one copy each of the proto-Y and proto-X, while the sex-reversed males carry two  
110 copies of the proto-X chromosome and no proto-Y. Using sex-reversed males allows us to  
111 control for the effect of sexually dimorphic gene expression on the inference of divergence  
112 between the proto-Y ( $III^M$ ) and proto-X. We used these data to test if the early evolution of a Y  
113 chromosome is dominated by chromosome-wide or gene-by-gene changes in expression.

114

115

## 116 **Results and Discussion**

117

### 118 **DNA sequence divergence between the proto-Y and proto-X chromosomes**

119

120 We used RNA-seq data to identify genetic variants (SNPs and small indels) within genes in  
121 genotypic ( $III^M/III$ ) and sex-reversed ( $III/III$ ) male house flies (Son et al. 2019). We found that  
122 the genotypic males have an excess of heterozygosity on the third chromosome, relative to the  
123 sex-reversed males (Figure 1;  $P < 10^{-16}$  in a Wilcoxon rank sum test comparing genes on the  
124 third chromosome with genes on the other chromosomes). This is consistent with a previous  
125 comparison between females and  $III^M$  males (Meisel et al. 2017), and it suggests that the

126 sequences of genes on the III<sup>M</sup> proto-Y chromosome are differentiated from the copies on the  
127 proto-X (i.e., the standard third chromosome).

128  
129 We would expect that there would be a similar level of heterozygosity on the ancestral X  
130 chromosome in the genotypic males (X/X; III<sup>M</sup>/III) and sex-reversed males (X/X; III/III) due to  
131 the presence of two copies of the X chromosome in both genotypes. However, the III<sup>M</sup> males  
132 have elevated heterozygosity on the X chromosome (Figure 1;  $P = 8.32 \times 10^{-13}$  in a Wilcoxon rank  
133 sum test comparing the X chromosome with chromosomes I, II, IV, and V). This was also  
134 observed in a comparison between females and III<sup>M</sup> males (Meisel et al. 2017), and the cause of  
135 the elevated X chromosome heterozygosity in III<sup>M</sup> males remains unresolved.

### 136 137 **Gene expression divergence between the proto-Y and proto-X chromosomes**

138  
139 Elevated heterozygosity on the third chromosome in genotypic (III<sup>M</sup>/III) males relative to sex-  
140 reversed (III/III) males suggests that the DNA sequences of the house fly III<sup>M</sup> proto-Y  
141 chromosome is differentiated from the standard third (proto-X) chromosome even if the proto-Y  
142 and proto-X chromosomes have similar morphology and gene content (Boyes et al. 1964;  
143 Hediger et al. 1998; Meisel et al. 2017). We hypothesized that X-Y sequence differences could  
144 contribute to expression differentiation between the proto-Y and the proto-X chromosomes. To  
145 test this hypothesis, we quantified differential gene expression between the proto-X and proto-Y  
146 chromosome copies of the third chromosome using the RNA-seq data described above and new  
147 Oxford Nanopore long read sequencing data.

148  
149 We quantified ASE of genes in genotypic (III<sup>M</sup>/III) and sex-reversed (III/III) males on the third  
150 (proto-sex) chromosome (Figure 2) and the other chromosomes (Supplementary Figure 1). We  
151 measured ASE as the proportion of iterations in an MCMC simulation in which the expression of  
152 a focal haplotype is estimated as  $>0.5$  (see Materials and Methods). The proportions of iterations  
153 with focal haplotypes  $>0.5$  were overrepresented at five points in the histograms (0, 0.25, 0.5,  
154 0.75, and 1) both in genotypic and sex-reversed males (Figure 2 and Supplementary Figure 1).  
155 These proportions may be overrepresented because we only sampled two genotypes for our ASE  
156 analysis, which caused us to have a non-continuous distribution of proportions.

157  
158 The proportion of iterations with a focal haplotype  $>0.5$  gives a measure of ASE ranging from 0  
159 (extreme ASE in favor of one allele) to 1 (extreme ASE in favor of another allele), with 0.5  
160 indicating equal expression of both alleles. We divided our measures of ASE into five bins, with  
161 each bin capturing one of the five most common proportions (Figure 2 and Supplementary  
162 Figure 1): 1) extreme ASE with a value between 0 and 0.125, 2) moderate ASE with a value  
163 between 0.125 and 0.375, 3) no ASE with a value between 0.375 and 0.625, 4) moderate ASE  
164 with a value between 0.625 and 0.875, and 5) extreme ASE with a value between 0.875 and 1. In  
165 the analysis below, we considered a gene to have ASE if it falls into one of the two bins of  
166 extreme ASE, and genes in the no ASE bin were classified as not having no allele-specific  
167 expression. Genes with moderate ASE were excluded in order to be conservative about ASE  
168 assignment.

169  
170 If the III<sup>M</sup> proto-Y chromosome is differentiated in gene expression from its homologous III  
171 proto-X chromosome because of differences in *cis*-regulatory alleles across the entire third

172 chromosome, then we expect a higher fraction of genes with ASE on the third chromosome in  
173 the genotypic ( $III^M/III$ ) males than in the sex-reversed ( $III/III$ ) males. In contrast to that  
174 expectation, we did not find an excess of genes with ASE in genotypic males compared to ASE  
175 genes in sex-reversed males on the third chromosome relative to other chromosomes (Figure 3A  
176 and Supplementary Table 1; Fisher's exact test,  $P = 0.6996$ ). This result suggests that the  $III^M$   
177 proto-Y chromosome is not broadly differentiated in *cis*-regulatory alleles from the standard  
178 third (proto-X) chromosome. This provides evidence that the early stages of Y chromosome  
179 evolution do not involve chromosome-wide changes in gene regulation via an excess of *cis*-  
180 regulatory mutations.

181  
182 We next identified individual genes with differences in ASE between genotypic ( $III^M/III$ ) and  
183 sex-reversed ( $III/III$ ) males. There are 95 genes with extreme ASE in the genotypic males and no  
184 ASE in the sex-reversed males on the third chromosome (Supplementary Table 2). These genes  
185 could have ASE in  $III^M$  males because of differences in *cis* regulatory sequences between the  
186  $III^M$  and standard third chromosome. To test whether the observed number of third chromosome  
187 genes with ASE in genotypic males and no ASE in sex-reversed males is in excess of a null  
188 expectation, we determined the number of third chromosome genes with no ASE in genotypic  
189 males and extreme ASE in sex-reversed males (i.e., the opposite of what we did above to find the  
190 first set of 95 genes). There are 76 genes with no ASE in the genotypic males and extreme ASE  
191 in the sex-reversed males on the third chromosome (Supplementary Table 2). To test if there is a  
192 significant excess of genes with ASE on the third chromosome in  $III^M$  males, we also identified  
193 241 genes on other chromosomes with ASE in genotypic males and no ASE in sex-reversed  
194 males, as well as 281 genes on other chromosomes with no ASE in genotypic males and ASE in  
195 sex-reversed males (Figure 3B and Supplementary Table 2). There is an excess of genes (95)  
196 with ASE in genotypic males and non-ASE in sex-reversed males compared to the number of  
197 genes (76) with non-ASE in genotypic males and ASE in sex-reversed males on the third  
198 chromosome, relative to the other chromosomes (Figure 3B and Supplementary Table 2; Fisher's  
199 exact test,  $P = 0.03467$ ). These results suggest that, while the  $III^M$  proto-Y chromosome is not  
200 broadly differentiated in *cis*-regulatory sequences from the standard third (proto-X)  
201 chromosome, there is an excess of individual genes with *cis*-regulatory differences between the  
202  $III^M$  proto-Y and its homologous proto-X chromosome.

### 203 204 **Up-regulation of the Y-allele and sex-biased expression**

205  
206 Male-beneficial/female-detrimental sexually antagonistic alleles are expected to accumulate on a  
207 Y chromosome (Rice 1984). These sexually antagonistic polymorphisms can favor the inhibition  
208 of recombination between the male-determining gene and any loci with sexually antagonistic  
209 alleles, thereby causing X-Y divergence (van Doorn and Kirkpatrick 2007; van Doorn and  
210 Kirkpatrick 2010). One way for alleles to have sexually antagonistic effects is if they are  
211 expressed at a level that is beneficial to one sex and deleterious in the opposite sex (Parsch and  
212 Ellegren 2013). Alternatively, differential expression of the Y-linked allele from the homologous  
213 allele on the X chromosome could be favored after protein-coding sequence divergence between  
214 the X and Y alleles that resulted from the fixation of male-beneficial sexually antagonistic alleles  
215 in the coding sequence of the Y-linked copy (Mank 2017). In both cases, we expect differential  
216 expression between X and Y alleles.

217



218 To test for expression divergence between X and Y copies that are likely to have sex-specific  
219 effects, we simultaneously investigated ASE and sex-biased gene expression. Specifically, we  
220 tested if genes on the third chromosome with ASE in the genotypic (III<sup>M</sup>/III) males and no ASE  
221 in the sex-reversed (III/III) males are differentially expressed between genotypic and sex-  
222 reversed males. We previously showed that genes with “discordant sex-biased expression” (i.e.,  
223 opposite sex-biased expression) between the genotypic and sex-reversed males are over-  
224 represented on the third chromosome (Son et al. 2019), suggesting divergence of *cis*-regulatory  
225 alleles between the III<sup>M</sup> (proto-Y) and standard third (proto-X) chromosomes. However, we did  
226 not previously determine which alleles (proto-Y or proto-X copies) are responsible for the  
227 expression differences between genotypic and sex-reversed males.

228  
229 Using our ASE results, we found one gene (LOC101899975, encoding XM\_011293910.2 and  
230 XM\_011293909.2) with discordant sex-biased gene expression out of the 95 genes on the third  
231 chromosome with ASE in the genotypic (III<sup>M</sup>/III) males and no ASE in the sex-reversed (III/III)  
232 males. This gene is homologous to *dynein assembly factor 5, axonemal* (human gene *DNAAF5*  
233 and *Drosophila melanogaster* gene *HEATR2*). The gene, which we refer to as *Musca domestica*  
234 *HEATR2* (*Md-HEATR2*), is expected to encode a protein that functions in flagellated sperm  
235 motility (Diggle et al. 2014), and it has strong testis-biased expression in *D. melanogaster*  
236 (Chintapalli et al. 2007). *Md-HEATR2* has male-biased expression in genotypic males and  
237 female-biased expression in sex-reversed males (Son et al. 2019), suggesting that expression  
238 differences between the III<sup>M</sup> proto-Y and the standard third (proto-X) chromosome cause the  
239 male-biased expression of the gene in the genotypic males.

240  
241 With haplotypes estimated by IDP-ASE, we identified three diagnostic variant sites for ASE  
242 within *Md-HEATR2* (Figure 4A), which are all synonymous SNPs. The genotypic (III<sup>M</sup>/III)  
243 males are heterozygous and the sex-reversed (III/III) males are homozygous at all diagnostic  
244 sites. We inferred the allele on the standard third chromosome as the one in common between  
245 genotypic and sex-reversed males, and the III<sup>M</sup> allele as the one unique to genotypic males at  
246 each diagnostic variant site. *Md-HEATR2* is expressed higher in III<sup>M</sup> genotypic males than in  
247 sex-reversed males (Figure 4A). In the III<sup>M</sup> genotypic males, the III<sup>M</sup> (Y-linked) alleles are  
248 expressed higher than the X-linked alleles, indicating that the Y-linked alleles are associated with  
249 the up-regulation of the gene in III<sup>M</sup> genotypic males relative to sex-reversed males (Figure 4A).  
250 The copy of *Md-HEATR2* on the III<sup>M</sup> proto-Y chromosome is therefore up-regulated relative to  
251 the proto-X copy.

252  
253 The evolutionary divergence of the proto-X and proto-Y copies of *Md-HEATR2* could constitute  
254 an early stage of X-Y differentiation before chromosome-wide X-Y differentiation occurs  
255 (Bachtrog 2013). Young Y chromosomes have very similar gene content as their ancestral  
256 autosomes, in contrast to old Y chromosomes that have only retained genes with male-specific  
257 functions or recruited genes associated with testis expression from other autosomes (Koerich et  
258 al. 2008; Kaiser et al. 2011; Mahajan and Bachtrog 2017). Our results suggest that changes in the  
259 expression of individual Y-linked genes that were retained from the ancestral autosome could  
260 have important phenotypic effects during early Y chromosome evolution, as opposed to  
261 chromosome-scale divergence of the proto-Y chromosome from its homologous proto-X  
262 chromosome (Zhou and Bachtrog 2012).

263

264 Using Nanopore long read sequencing data, we examined 1,273 base pairs upstream of *Md-*  
265 *HEATR2* to identify diagnostic sites that could be responsible for regulating the expression  
266 differences between the proto-X and proto-Y alleles. We chose that distance because it includes  
267 the first variable site we could identify on the scaffold containing *Md-HEATR2* in our Nanopore  
268 data (i.e., including a larger region would not provide any additional information). We found  
269 twelve variable sites with different variants (SNPs and small indels) between genotypic (III<sup>M</sup>/III)  
270 and sex-reversed (III/III) males (Figure 4B). We next examined whether these sites are located  
271 within a potential transcription factor (TF) binding region. We found five TF binding regions  
272 predicted upstream of *Md-HEATR2* using the ‘Tfsitescan’ tool in the ‘object-oriented  
273 Transcription Factors Database (ooTFD)’ (Ghosh 1999). However, none of the twelve variable  
274 sites are found within any predicted TF binding regions (Figure 4C). Further work is needed to  
275 determine how the differential expression of the proto-X and proto-Y copies of *Md-HEATR2* is  
276 regulated.

277  
278 If alleles have sexually antagonistic effects (e.g., beneficial to males and deleterious to females),  
279 then selection on these alleles could drive sex chromosome turnover if they are tightly linked to a  
280 new sex-determining gene (Orzack et al. 1980; van Doorn and Kirkpatrick 2007; Roberts et al.  
281 2009; van Doorn and Kirkpatrick 2010). The genetic linkage between sexually antagonistic  
282 alleles and the new sex-determining locus could favor restricted or suppressed recombination  
283 between the proto-Y and proto-X chromosomes in that linked region, triggering additional X-Y  
284 differentiation (Bachtrog 2013). The expression of *Md-HEATR2* could be under sexually  
285 antagonistic selection because it functions in flagellated sperm motility (Diggle et al. 2014). *Md-*  
286 *HEATR2* has male-biased expression in abdominal tissue (Son et al. 2019), consistent with a  
287 function in spermatogenesis. Axonemal dynein is important for male fertility by affecting sperm  
288 motility in *Drosophila* (Kurek et al. 1998; Carvalho et al. 2000), suggesting that it may be  
289 beneficial to male fitness to have higher expression of *Md-HEATR2*. In addition, investment in  
290 expressing the gene in females could be costly, possibly because of the gene’s other functions in  
291 mechanosensory neurons (Diggle et al. 2014). Therefore, the up-regulation of *Md-HEATR2* in  
292 XY males due to high expression of the proto-Y copy could be consistent with sexually  
293 antagonism playing an important role in the early stage of X-Y differentiation at individual genes  
294 in house fly.

## 295 296 **Conclusions**

297  
298 We investigated gene sequence and expression differences between the III<sup>M</sup> proto-Y and its  
299 homologous proto-X chromosome to determine how a very young Y chromosome has been  
300 differentiated from its homologous X chromosome shortly after it was formed. To those ends, we  
301 used genotypic (III<sup>M</sup>/III) and sex-reversed (III/III) males because they are phenotypically almost  
302 the same but differ in the proto-sex chromosomes they carry (Hediger et al. 2010; Son et al.  
303 2019). We found increased heterozygosity on the III<sup>M</sup> proto-Y chromosome in genotypic males  
304 relative to sex-reversed males, consistent with sequence divergence between the proto-Y and  
305 proto-X (Figure 1). There is not an excess of genes with ASE on the proto-sex chromosome in  
306 genotypic males compared to genes with ASE on the same chromosome in sex-reversed males  
307 (Figure 3A and Supplementary Table 1). In contrast, we found an excess of individual genes  
308 with ASE in the genotypic males and no ASE in the sex-reversed males on the proto-sex  
309 chromosome relative to the other chromosomes (Figure 3B and Supplementary Table 2).



310 However, the number of genes with ASE on the third chromosome only in genotypic males, and  
311 not in sex-reverse males, is small (<100, which is likely less than 5% of the entire chromosome).  
312 We identified one gene on the third chromosome (*Md-HEATR2*) with ASE in genotypic males,  
313 no ASE in sex-reversed males, and discordant sex-biased expression between genotypic and sex-  
314 reversed males (Figure 4). We hypothesize that expression divergence of *Md-HEATR2* could be  
315 an example of very early X-Y differentiation of individual genes that results from sexually  
316 antagonistic selection. Therefore, the house fly III<sup>M</sup> proto-Y chromosome is differentiated in  
317 gene sequence and expression from its homologous proto-X chromosome at individual genes,  
318 but not chromosome wide. This suggests that the earliest stages of Y chromosome evolution  
319 consist of gene-by-gene, rather than chromosome-scale, changes in gene expression.

320

321

## 322 **Materials and Methods**

323

### 324 **Fly strain**

325

326 We analyzed RNA-seq data and performed Oxford Nanopore sequencing on a house fly strain  
327 that allows for identification of genotypic (III<sup>M</sup>/III) males and sex-reversed (III/III) males  
328 (Hediger et al. 2010). This is because the standard third chromosome (III) in this strain has the  
329 recessive mutations *pointed wing* (*pw*) and *brown body* (*bwb*). Sex-reversed males (and normal  
330 females) have both mutant phenotypes, whereas genotypic males are wild-type for both  
331 phenotypes because the III<sup>M</sup> chromosome has the dominant wild-type alleles. The RNA-seq data  
332 that we analyzed (available at NCBI GEO accession GSE126689) comes from a previous study  
333 that used double-stranded RNA (dsRNA) targeting *Md-tra* to create sex-reversed phenotypic  
334 males that have a female genotype without a proto-Y chromosome (Son et al. 2019). We  
335 compared the sex-reversed males to genotypic males that received a sham treatment of dsRNA  
336 targeting GFP. This comparison allows us to investigate genes that have different sex-biased  
337 expression in genotypic and sex-reversed males (Son et al. 2019). We used genotypic males and  
338 sex-reversed males from the same strain that were subjected to the same treatment for genome  
339 sequencing using the Oxford Nanopore long read technology.

340

### 341 **Oxford Nanopore sequencing**

342

343 We performed Oxford Nanopore sequencing of one genotypic (III<sup>M</sup>/III) male and one sex-  
344 reversed (III/III) male created in the same strain and using the same *Md-tra* dsRNA treatment as  
345 a previous RNA-seq study (Son et al. 2019). DNA was isolated with a phenol/chloroform  
346 protocol. A single genotypic male and a single sex-reversed male with detached wings were each  
347 transferred to a 1.5 mL Eppendorf tube with 0.5mL homogenization buffer (4.1 g sucrose, 15 mL  
348 1M Tris-HCl pH 8.0, 0.5M EDTA, 100 mL dH<sub>2</sub>O) and then homogenized using pestles set into a  
349 tissue grinder homogenizer. To each tube we added 40 uL of 10% SDS and 2.5 uL of 10mg/mL  
350 Proteinase K, and then we incubated the tube at 65°C for 30 min. We next added 2 uL of 4  
351 mg/mL RNase to each tube and incubated at 37°C for 15 min. We added 48 uL of 5M KAc to  
352 each tube and placed on ice for 30 min. Then we centrifuged the tubes at 14000 rpm for 10 min  
353 at 4°C, and the supernatant was transferred into a new tube using a wide-bore pipette tip (all  
354 subsequent steps of transfer and mixing during DNA extraction were also done with wide-bore  
355 pipette tips to prevent DNA shearing). We added 250 uL phenol and 250 uL chloroform to the

356 extracted supernatant in the new tube, mixed briefly, spun at 14000 rpm for 15 min at 4°C, and  
357 then transferred the supernatant into a new tube. We next added 500 uL chloroform to the  
358 supernatant in the new tube, mixed well, and spun a 14000 rpm for 5 min at 4°C. We then  
359 transferred the supernatant into a new tube. We added 40 uL of 3M NaAc and 800 uL of 95%  
360 ethanol to the supernatant in the new tube, mixed briefly, spun at 14000 rpm for 15 min at 4°C,  
361 and then carefully poured off all supernatant. We next added 800 uL of 70% ethanol to the  
362 remaining pellet, mixed briefly to wash the pellet, spun at 14000 rpm for 15 min at 4°C, removed  
363 the supernatant, and then resuspended the pellet in 30 uL of nuclease-free water.

364  
365 Oxford Nanopore Sequencing libraries were prepared with the 1D genomic DNA Ligation kit  
366 (SQK-LSK109, Oxford Nanopore), following the manufacturer's protocol. DNA from the  
367 genotypic male and sex-reversed male (see above) was used to create a separate sequencing  
368 library for each genotype. Following the manufacturer's protocol, 15 uL of each library, along  
369 with sequencing buffer and loading beads (totaling 75 uL), were loaded onto a R9.4 flow cell  
370 until no pores were available on a MinION sequencer (Oxford Nanopore). The libraries from the  
371 genotypic and sex-reversed males were run on separate flow cells. Base calling was performed  
372 using the Guppy pipeline software version 3.1.5 (Oxford Nanopore) with parameters (--  
373 calib\_detect --qscore\_filtering --min\_qscore 10). The base called reads were aligned to the house  
374 fly genome assembly v2.0.2 (Scott et al. 2014) using Minimap2 version 2.17 with the "--ax map-  
375 ont" parameter (Li 2018).

### 376 **Variant calling**

377  
378 We used available RNA-seq data (Son et al. 2019) to identify genetic variants (SNPs and small  
379 insertions/deletions) that differentiate the III<sup>M</sup> proto-Y chromosome from the standard third  
380 (proto-X) chromosome, and then we tested if III<sup>M</sup> males have elevated heterozygosity on the  
381 third chromosome as compared to sex-reversed males (Meisel et al. 2017). We used the Genome  
382 Analysis Toolkit (GATK) pipeline for calling variants in the RNA-seq data from the *Md-tra*  
383 RNAi experiment in (Son et al. 2019), following the best practices for SNP and  
384 insertion/deletion (indel) calling on RNA-seq data (McKenna et al. 2010; Meisel et al. 2017). We  
385 used STAR (Dobin et al. 2013) to align reads from three genotypic (III<sup>M</sup>/III) male libraries and  
386 three sex-reversed (III/III) male libraries to the reference assembly v2.0.2 (Scott et al. 2014). The  
387 aligned reads were used to generate a new reference genome index from the detected splice  
388 junctions in the first alignment run, and then a second alignment was performed with the new  
389 reference. We next marked duplicate reads from the same RNA molecule and used the GATK  
390 tool 'SplitNCigarReads' to reassign mapping qualities to 60 with the  
391 'ReassignOneMappingQuality' read filter for alignments with a mapping quality of 255. Indels  
392 were detected and realigned with 'RealignerTargetCreator' and 'IndelRealigner'. The realigned  
393 reads were used for base recalibration with 'BaseRecalibrator' and 'PrintReads'. The base  
394 recalibration was performed in three sequential iterations in which recalibrated and filtered reads  
395 were used to train the next round of base recalibration, at which point there were no beneficial  
396 effects of additional base recalibration as verified by 'AnalyzeCovariates'. We next used the  
397 recalibrated reads from all three replicates of genotypic and sex-reversed males to call variants  
398 using 'HaplotypeCaller' with emission and calling confidence thresholds of 20. We applied  
399 'genotypeGVCFs' to the variant calls from the two types of males for joint genotyping, and then  
400 we filtered the variants using 'VariantFiltration' with a cluster window size of 35 bp, cluster size  
401

402 of 3 SNPs,  $FS > 20$ , and  $QD < 2$ . The final variant calls were used to identify heterozygous  
403 variants within genes using the coordinates from the genome sequencing project, annotation  
404 release 102 (Scott et al. 2014). We measured relative heterozygosity within each gene in  
405 genotypic (III<sup>M</sup>/III) and sex-reversed (III/III) males as the number of heterozygous variants in  
406 genotypic males for a given gene ( $h_G$ ) divided by the total number heterozygous variants in both  
407 genotypic and sex-reversed males ( $h_{SR}$ ), times one hundred:  $100h_G/(h_G + h_{SR})$ .

408  
409 For the variant calling from Nanopore long reads, the base called reads were indexed using fast5  
410 files with the ‘index’ module of Nanopolish version 0.11.1 (Quick et al. 2016), and they were  
411 aligned with Minimap2 version 2.17 (Li 2018) to house fly genome assembly v2.0.2 (Scott et al.  
412 2014). The aligned and raw reads were used to call variants using the “variants” module of  
413 Nanopolish version 0.11.1 with the “--ploidy 2” parameter (Quick et al. 2016). We used a python  
414 script ‘nanopolish\_makerange.py’ provided in the package to split the genome into 50 kb  
415 segments because it was recommended to use the script for large datasets with genome size more  
416 than 50 kb.

### 417 **Allele-specific expression**

418  
419 Diploid species can have two alleles at a locus, one of which was inherited maternally and the  
420 other paternally. The maternal and paternal alleles can be expressed unequally in the diploid,  
421 which is called allele-specific expression (ASE). We investigated if there is elevated ASE on the  
422 third chromosome in males carrying one III<sup>M</sup> proto-Y and one proto-X chromosome compared to  
423 sex-reversed males with two proto-X chromosomes. To do this, we implemented the IDP-ASE  
424 tool at the gene level with house fly genome annotation release 102 (Scott et al. 2014), following  
425 the developers’ recommended analysis steps (Deonovic et al. 2016). We first prepared  
426 information on the number and locations of variants within each gene (SNPs and small indels),  
427 as well as read counts at each variant location (see above). The IDP-ASE software was supplied  
428 with raw reads and aligned reads created by RNA-seq (Son et al. 2019) and Nanopore  
429 sequencing, and variant calls created only by GATK because Nanopore sequencing reads of each  
430 library (genotypic male and sex-reversed male) had less than  $10 \times$  coverage across the house fly  
431 genome (i.e., too low for reliable variant calling).

432  
433 The prepared data from each gene was next run in an MCMC (Markov chain Monte Carlo)  
434 sampling simulation to estimate the haplotype within each gene with a Metropolis-Hastings  
435 sampler (Bansal et al. 2008). Next, the software estimates the proportion of each estimated  
436 haplotype that contributes to the total expression of the gene ( $\rho$ ) from each iteration using slice  
437 sampling (Neal and others 2003). A value of  $\rho=0.5$  indicates equal expression between two  
438 alleles, whereas  $\rho<0.5$  or  $\rho>0.5$  indicates ASE. The MCMC sampling was run with a 1000  
439 iteration burn-in followed by at least 500 iterations where data were recorded. The actual number  
440 of iterations was automatically adjusted by the software during the simulation to produce the best  
441 simulation output for quantifying ASE within a gene. The IDP-ASE simulation generated a  
442 distribution of  $\rho$  for each gene across all post-burn-in iterations, and then it calculated the  
443 proportion of iterations with  $\rho > 0.5$ . This proportion was used to estimate the extent of ASE for  
444 each gene. For example, if all iterations for a gene have  $\rho > 0.5$ , then the proportion is 1 and the  
445 gene has strong evidence for ASE of one allele. Similarly, if all iterations for a gene have  $\rho <$   
446 0.5, then the proportion is 0 and the gene has strong evidence for ASE of the other allele. In  
447

448 contrast, if half of the iterations have  $\rho > 0.5$  and the other half have  $\rho < 0.5$ , then the proportion  
449 is 0.5 and there is not any evidence for ASE. To classify whether genes have ASE or not, we  
450 considered only genes with total RNA-seq read counts above 10.

451  
452 We used the output of IDP-ASE to compare expression of the III<sup>M</sup> (proto-Y) and III (proto-X)  
453 alleles in genotypic males. IDP-ASE only quantifies ASE within bi-allelic loci, so we only  
454 included genes with heterozygous sites within transcripts in genotypic (III<sup>M</sup>/III) or sex-reversed  
455 (III/III) males. In addition, we removed heterozygous variants with the same genotype in  
456 genotypic and sex-reversed males because they do not allow us discriminate between the proto-Y  
457 and proto-X alleles. Removing these variants may have also sped up the simulation times, but  
458 this was not rigorously investigated. To discriminate between the III<sup>M</sup> and III alleles, we used  
459 haplotypes estimated during IDP-ASE runs and genotypes inferred from GATK for genotypic  
460 (III<sup>M</sup>/III) and sex-reversed (III/III) males. For example, using genotypes called using GATK  
461 from the RNA-seq data, we first identified sites with heterozygous alleles in genotypic males and  
462 homozygous alleles in sex-reversed males. Next, we inferred the allele in common between  
463 genotypic and sex-reversed as the III allele, and the other allele that is unique to genotypic males  
464 as the III<sup>M</sup> allele. Lastly, we matched those sites to the haplotypes estimated by IDP-ASE to  
465 quantify ASE within each genotype.

466  
467  
468

#### 469 **Acknowledgements and funding information**

470 This work was supported by Grant-in-Aid of Research from the National Academy of Sciences,  
471 administered by Sigma Xi, The Scientific Research Society (grant number G2018100198487895  
472 to J.H.S. and R.P.M.) and by the National Science Foundation (grant numbers OISE-1444220  
473 and DEB-1845686 to R.P.M.). The Oxford Nanopore long reads data used in the study are  
474 available from the National Center for Biotechnology Information Sequence Read Archive under  
475 BioProject accession PRJNA620357 (BioSample accessions SAMN14518459 for sex-reversed  
476 males and SAMN14518460 for genotypic males).

477  
478  
479

## 480 **Figure Legends**

481

482 **Figure 1.** Elevated heterozygosity on the third and X chromosomes in genotypic ( $III^M/III$ ) males  
483 relative to sex-reversed ( $III/III$ ) males. The boxplots show the distributions of the percentages of  
484 heterozygous variants within genes on each chromosome in the genotypic males relative to the  
485 sex-reversed males. Values more than 50% indicate the increased heterozygosity in genotypic  
486 ( $III^M/III$ ) males, and less than 50% is increased heterozygosity in sex-reversed males. The  
487 median across all autosomes is represented by a dashed line.

488

489 **Figure 2.** Histograms of ASE for third chromosome genes in (A) genotypic ( $III^M/III$ ) and  
490 (B) sex-reversed ( $III/III$ ) males. If a gene is expressed equally between the X and Y alleles, the  
491 proportion of focal haplotypes is 0.5; if a gene has ASE, the proportion is greater or less than 0.5.

492

493 **Figure 3.** (A) Proportions of genes with ASE in genotypic ( $III^M$ ) and sex-reversed (SR) males on  
494 each chromosome. (B) Proportions of genes with ASE in genotypic males and non-ASE in sex-  
495 reversed males on the third chromosome and all other chromosomes (left two bars). Proportions  
496 of genes with non-ASE in genotypic and ASE in sex-reversed males on the third chromosome  
497 and all other chromosomes (right two bars).

498

499 **Figure 4.** (A) Diagnostic variable sites for allele-specific expression (ASE) of the *Md-HEATR2*  
500 gene based on haplotypes estimated in IDP-ASE; fragments per million mapped reads (FPM).  
501 (B) Variable sites that differ between genotypic ( $III^M$ ) males and sex-reversed males across 1,273  
502 base pairs upstream of *Md-HEATR2* using Oxford Nanopore long reads only. The variable sites  
503 are marked as triangles with their coordinate as positions in scaffold. (C) Transcription factor  
504 (TF) binding motifs predicted within 1,273 base pairs upstream of *Md-HEATR2*.



## 505 **References**

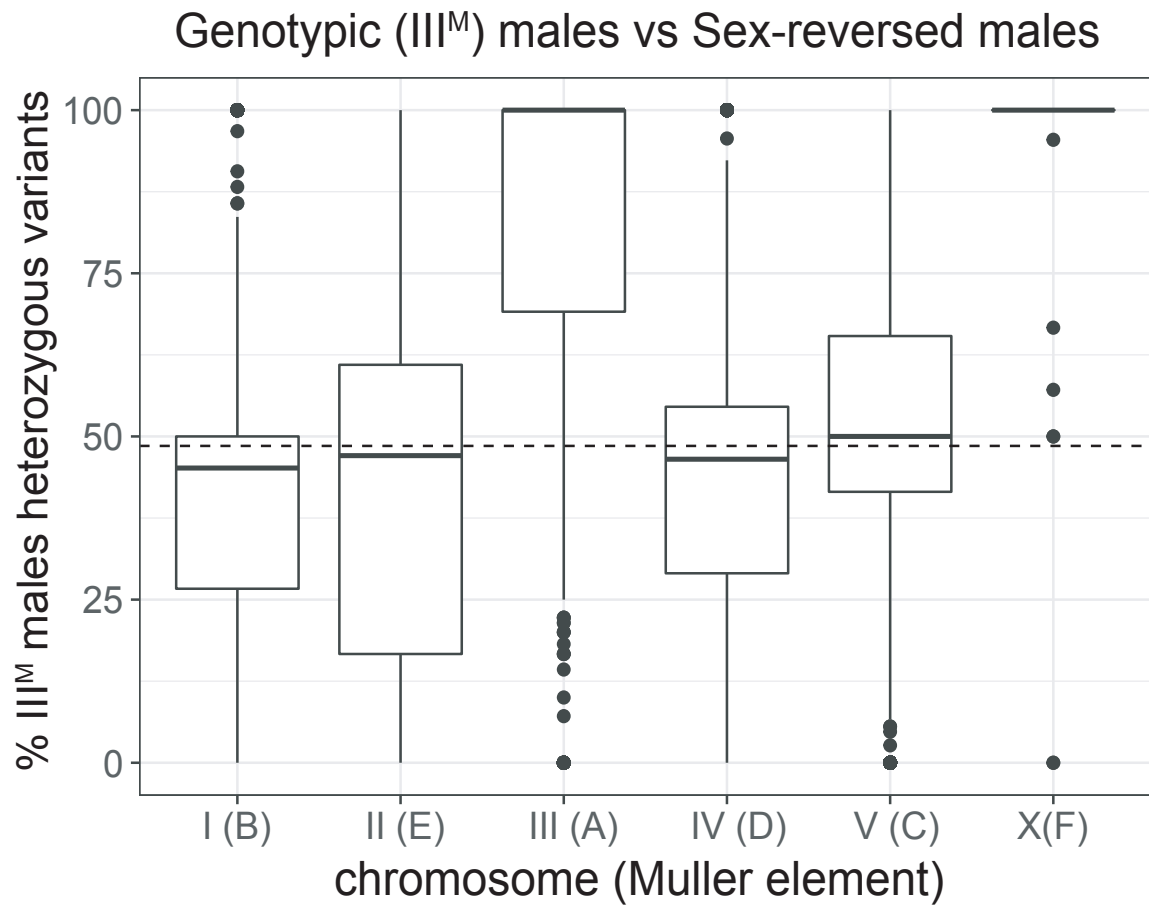
- 506  
507 Bachtrog D. 2013. Y-chromosome evolution: emerging insights into processes of Y-chromosome  
508 degeneration. *Nat Rev Genet.* 14(2):113.  
509
- 510 Bachtrog D, Mank JE, Peichel CL, Kirkpatrick M, Otto SP, Ashman T-L, Hahn MW, Kitano J,  
511 Mayrose I, Ming R, et al. 2014. Sex determination: why so many ways of doing it? *PLoS Biol.*  
512 12(7):e1001899.  
513
- 514 Bansal V, Halpern AL, Axelrod N, Bafna V. 2008. An MCMC algorithm for haplotype assembly  
515 from whole-genome sequence data. *Genome Res.* 18(8):1336–1346.  
516
- 517 Bergero R, Qiu S, Forrest A, Borthwick H, Charlesworth D. 2013. Expansion of the pseudo-  
518 autosomal region and ongoing recombination suppression in the *Silene latifolia* sex  
519 chromosomes. *Genetics.* doi:10.1534/genetics.113.150755.  
520
- 521 Beukeboom LW, Perrin N. 2014. The evolution of sex determination. Oxford University Press,  
522 USA.  
523
- 524 Boyes JW, Corey MJ, Paterson HE. 1964. Somatic chromosomes of higher diptera: IX.  
525 Karyotypes of some muscid species. *Can J Zool.* 42(6):1025–1036.  
526
- 527 Bull JJ. 1983. Evolution of sex determining mechanisms. The Benjamin/Cummings Publishing  
528 Company, Inc.  
529
- 530 Carvalho AB, Lazzaro BP, Clark AG. 2000. Y chromosomal fertility factors kl-2 and kl-3 of  
531 *Drosophila melanogaster* encode dynein heavy chain polypeptides. *Proc Natl Acad Sci.*  
532 97(24):13239–13244.  
533
- 534 Charlesworth B, Charlesworth D. 2000. The degeneration of Y chromosomes. *Philos Trans R*  
535 *Soc London Ser B Biol Sci.* 355(1403):1563–1572.  
536
- 537 Charlesworth D. 2018. Does sexual dimorphism in plants promote sex chromosome evolution?  
538 *Environ Exp Bot.* doi:10.1016/j.envexpbot.2017.11.005.  
539
- 540 Charlesworth D, Charlesworth B, Marais G. 2005. Steps in the evolution of heteromorphic sex  
541 chromosomes. *Heredity (Edinb).* 95(2):118.  
542
- 543 Chintapalli VR, Wang J, Dow JAT. 2007. Using FlyAtlas to identify better *Drosophila*  
544 *melanogaster* models of human disease. *Nat Genet.* doi:10.1038/ng2049.  
545
- 546 Darolti I, Wright AE, Sandkam BA, Morris J, Bloch NI, Farré M, Fuller RC, Bourne GR, Larkin  
547 DM, Breden F, et al. 2019. Extreme heterogeneity in sex chromosome differentiation and dosage  
548 compensation in livebearers. *Proc Natl Acad Sci U S A.* doi:10.1073/pnas.1905298116.  
549
- 550 Deonovic B, Wang Y, Weirather J, Wang X-J, Au KF. 2016. IDP-ASE: haplotyping and

- 551 quantifying allele-specific expression at the gene and gene isoform level by hybrid sequencing.  
552 *Nucleic Acids Res.* 45(5):e32--e32.  
553
- 554 Diggle CP, Moore DJ, Mali G, zur Lage P, Ait-Lounis A, Schmidts M, Shoemark A, Garcia  
555 Munoz A, Halachev MR, Gautier P, et al. 2014. HEATR2 Plays a Conserved Role in Assembly  
556 of the Ciliary Motile Apparatus. *PLoS Genet.* doi:10.1371/journal.pgen.1004577.  
557
- 558 Dobin A, Davis CA, Schlesinger F, Drenkow J, Zaleski C, Jha S, Batut P, Chaisson M, Gingeras  
559 TR. 2013. STAR: ultrafast universal RNA-seq aligner. *Bioinformatics.* 29(1):15–21.  
560
- 561 van Doorn GS, Kirkpatrick M. 2007. Turnover of sex chromosomes induced by sexual conflict.  
562 *Nature.* 449(7164):909.  
563
- 564 van Doorn GS, Kirkpatrick M. 2010. Transitions between male and female heterogamety caused  
565 by sex-antagonistic selection. *Genetics.* 186(2):629–645.  
566
- 567 Ghosh D. 1999. Object oriented transcription factors database (ooTFD). *Nucleic Acids Res.*  
568 doi:10.1093/nar/27.1.315.  
569
- 570 Gu L, Walters JR. 2017. Evolution of sex chromosome dosage compensation in animals: A  
571 beautiful theory, undermined by facts and bedeviled by details. *Genome Biol Evol.*  
572 doi:10.1093/gbe/evx154.  
573
- 574 Hamm RL, Meisel RP, Scott JG. 2015. The evolving puzzle of autosomal versus Y-linked male  
575 determination in *Musca domestica*. *G3 Genes, Genomes, Genet.* 5(3):371–384.  
576
- 577 Hediger M, Henggeler C, Meier N, Perez R, Saccone G, Bopp D. 2010. Molecular  
578 characterization of the key switch F provides a basis for understanding the rapid divergence of  
579 the sex-determining pathway in the housefly. *Genetics.* 184(1):155–170.  
580
- 581 Hediger M, Minet AD, Niessen M, Schmidt R, Hilfiker-Kleiner D, Çakir Ş, Nöthiger R,  
582 Dübendorfer A. 1998. The male-determining activity on the Y chromosome of the housefly  
583 (*Musca domestica* L.) Consists of separable elements. *Genetics.*  
584
- 585 Kaiser VB, Zhou Q, Bachtrog D. 2011. Nonrandom gene loss from the drosophila miranda neo-  
586 Y chromosome. *Genome Biol Evol.* doi:10.1093/gbe/evr103.  
587
- 588 Koerich LB, Wang X, Clark AG, Carvalho AB. 2008. Low conservation of gene content in the  
589 *Drosophila* Y chromosome. *Nature.* doi:10.1038/nature07463.  
590
- 591 Krasovec M, Kazama Y, Ishii K, Abe T, Filatov DA. 2019. Immediate Dosage Compensation Is  
592 Triggered by the Deletion of Y-Linked Genes in *Silene latifolia*. *Curr Biol.*  
593 doi:10.1016/j.cub.2019.05.060.  
594
- 595 Kurek R, Reugels AM, Glaätzer KH, Bünemann H. 1998. The Y chromosomal fertility factor  
596 Threads in *Drosophila hydei* harbors a functional gene encoding an axonemal dynein  $\beta$  heavy

- 597 chain protein. *Genetics*. 149(3):1363–1376.  
598
- 599 Li H. 2018. Minimap2: Pairwise alignment for nucleotide sequences. *Bioinformatics*.  
600 doi:10.1093/bioinformatics/bty191.  
601
- 602 Mahajan S, Bachtrog D. 2017. Convergent evolution of y chromosome gene content in flies. *Nat*  
603 *Commun*. doi:10.1038/s41467-017-00653-x.  
604
- 605 Mahajan S, Wei KHC, Nalley MJ, Gibilisco L, Bachtrog D. 2018. De novo assembly of a young  
606 *Drosophila* Y chromosome using single-molecule sequencing and chromatin conformation  
607 capture. *PLoS Biol*. doi:10.1371/journal.pbio.2006348.  
608
- 609 Mank JE. 2013. Sex chromosome dosage compensation: Definitely not for everyone. *Trends*  
610 *Genet*. doi:10.1016/j.tig.2013.07.005.  
611
- 612 Mank JE. 2017. The transcriptional architecture of phenotypic dimorphism. *Nat Ecol Evol*.  
613 doi:10.1038/s41559-016-0006.  
614
- 615 McKenna A, Hanna M, Banks E, Sivachenko A, Cibulskis K, Kernytsky A, Garimella K,  
616 Altshuler D, Gabriel S, Daly M, et al. 2010. The Genome Analysis Toolkit: a MapReduce  
617 framework for analyzing next-generation DNA sequencing data. *Genome Res*. 20(9):1297–1303.  
618
- 619 Meisel RP, Gonzales CA, Luu H. 2017. The house fly Y Chromosome is young and minimally  
620 differentiated from its ancient X Chromosome partner. *Genome Res*. 27(8):1417–1426.  
621 Neal RM, others. 2003. Slice sampling. *Ann Stat*. 31(3):705–767.  
622
- 623 Orzack SH, Sohn JJ, Kallman KD, Levin SA, Johnston R. 1980. Maintenance of the three sex  
624 chromosome polymorphism in the platyfish, *Xiphophorus maculatus*. *Evolution* (N Y).  
625 34(4):663–672.  
626
- 627 Parsch J, Ellegren H. 2013. The evolutionary causes and consequences of sex-biased gene  
628 expression. *Nat Rev Genet*. doi:10.1038/nrg3376.  
629
- 630 Quick J, Loman NJ, Duraffour S, Simpson JT, Severi E, Cowley L, Bore JA, Koundouno R,  
631 Dudas G, Mikhail A, et al. 2016. Real-time, portable genome sequencing for Ebola surveillance.  
632 *Nature*. doi:10.1038/nature16996.  
633
- 634 Rice WR. 1984. Sex chromosomes and the evolution of sexual dimorphism. *Evolution* (N Y).  
635 38(4):735–742.  
636
- 637 Rice WR. 1987. The accumulation of sexually antagonistic genes as a selective agent promoting  
638 the evolution of reduced recombination between primitive sex chromosomes. *Evolution* (N Y).  
639 41(4):911–914.  
640
- 641 Rice WR. 1996. Evolution of the Y sex chromosome in animals. *Bioscience*. 46(5):331–343.  
642 Roberts RB, Ser JR, Kocher TD. 2009. Sexual conflict resolved by invasion of a novel sex

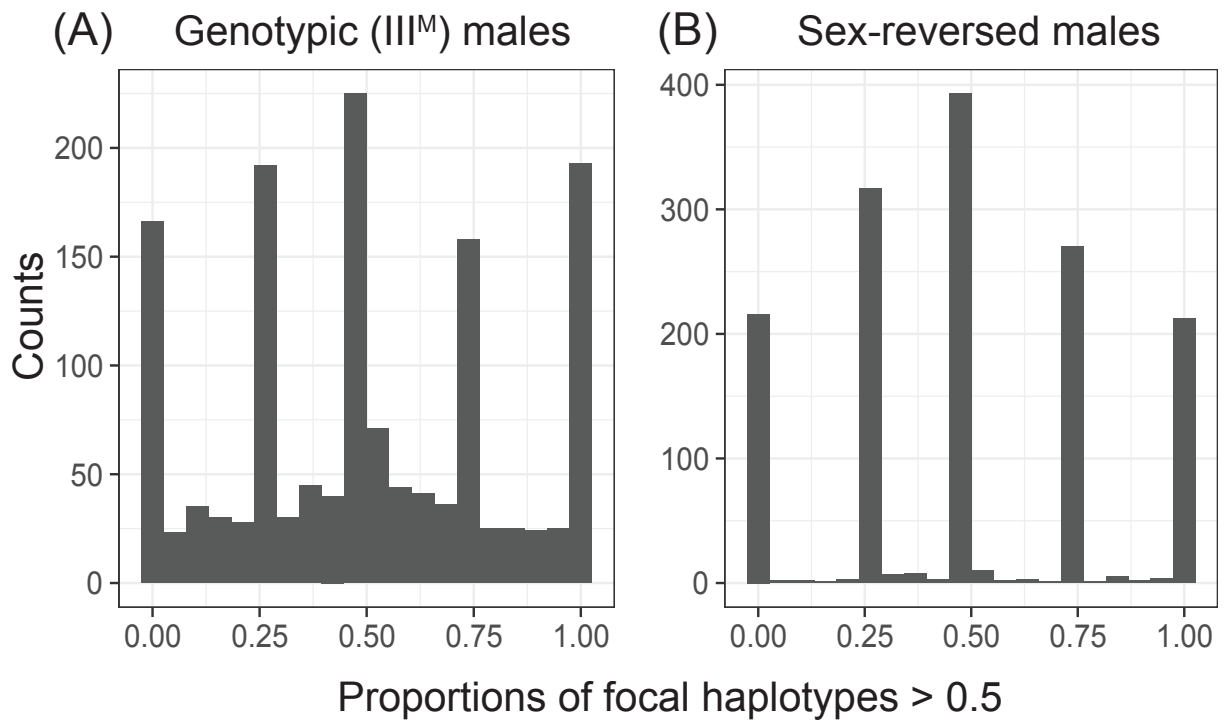
643 determiner in Lake Malawi cichlid fishes. *Science* (80- ). 326(5955):998–1001.  
644  
645 Scott JG, Warren WC, Beukeboom LW, Bopp D, Clark AG, Giers SD, Hediger M, Jones AK,  
646 Kasai S, Leichter CA, et al. 2014. Genome of the house fly, *Musca domestica* L., a global vector  
647 of diseases with adaptations to a septic environment. *Genome Biol.* 15(10):466.  
648  
649 Sharma A, Heinze SD, Wu Y, Kohlbrenner T, Morilla I, Brunner C, Wimmer EA, van de Zande  
650 L, Robinson MD, Beukeboom LW, et al. 2017. Male sex in houseflies is determined by *Mdmd*, a  
651 paralog of the generic splice factor gene *CWC22*. *Science* (80- ). 356(6338):642–645.  
652  
653 Skaletsky H, Kuroda-Kawaguchi T, Minx PJ, Cordum HS, Hillier L, Brown LG, Repping S,  
654 Pyntikova T, Ali J, Bieri T, et al. 2003. The male-specific region of the human Y chromosome is  
655 a mosaic of discrete sequence classes. *Nature.* 423(6942):825.  
656  
657 Son JH, Kohlbrenner T, Heinze S, Beukeboom LW, Bopp D, Meisel RP. 2019. Minimal effects  
658 of proto-Y chromosomes on house fly gene expression in spite of evidence that selection  
659 maintains stable polygenic sex determination. *Genetics.* doi:10.1534/genetics.119.302441.  
660  
661 Vicoso B. 2019. Molecular and evolutionary dynamics of animal sex-chromosome turnover. *Nat*  
662 *Ecol Evol.* doi:10.1038/s41559-019-1050-8.  
663  
664 Zhou Q, Bachtrog D. 2012. Chromosome-wide gene silencing initiates y degeneration in  
665 *drosophila*. *Curr Biol.* doi:10.1016/j.cub.2012.01.057.  
666  
667 Zhou Q, Zhang J, Bachtrog D, An N, Huang Q, Jarvis ED, Gilbert MTP, Zhang G. 2014.  
668 Complex evolutionary trajectories of sex chromosomes across bird taxa. *Science* (80- ).  
669 346(6215):1246338.  
670

671 **Figure 1**  
672



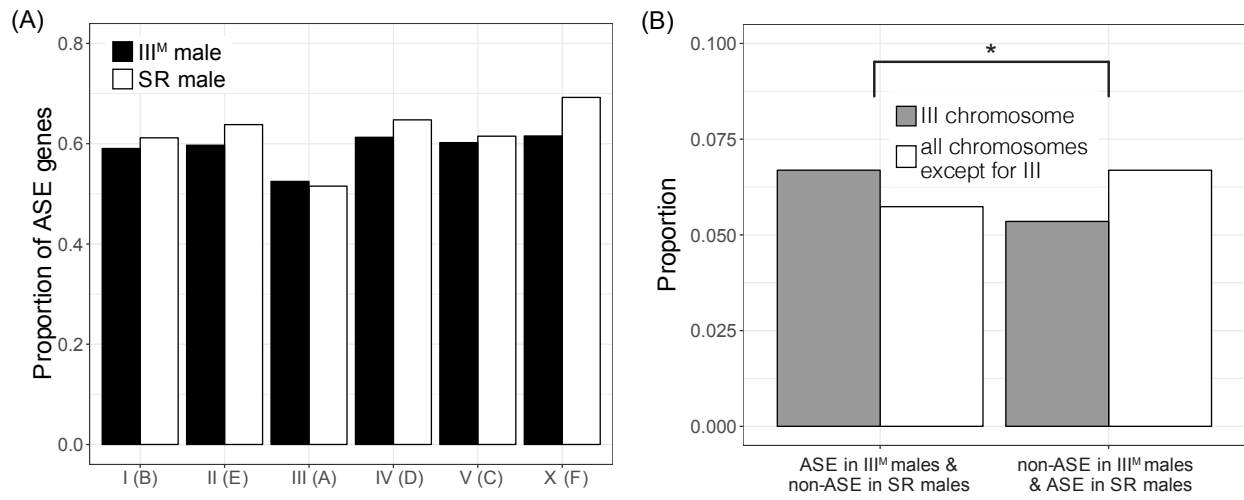


674 **Figure 2**



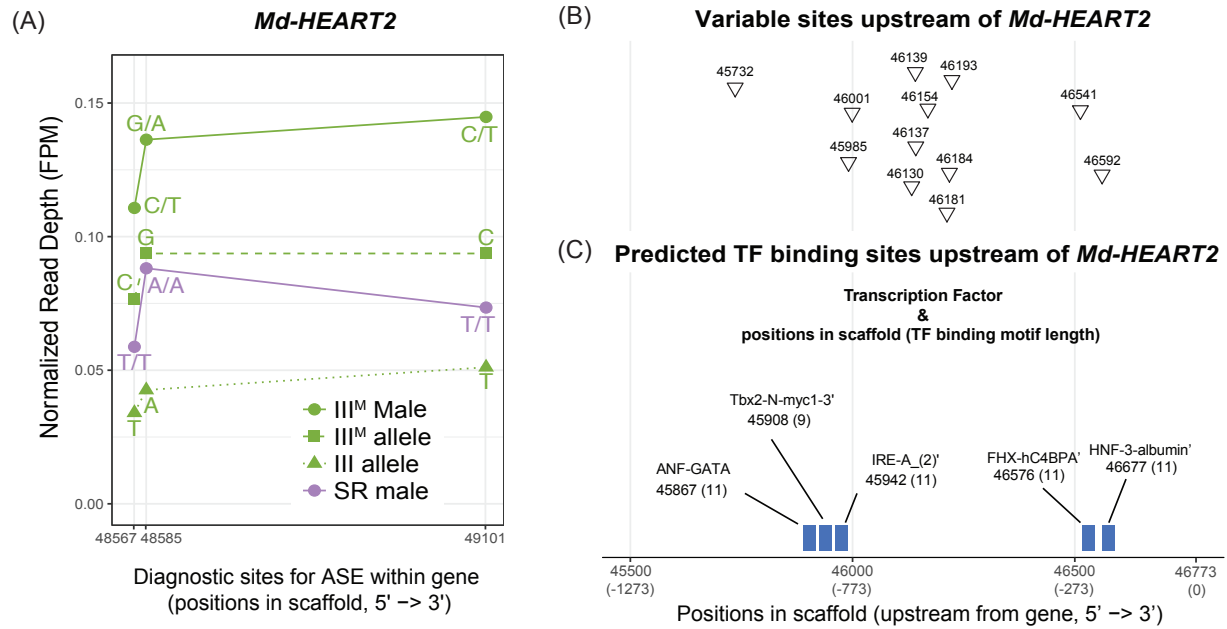
675

676 **Figure 3**  
677



678

679 **Figure 4**  
680



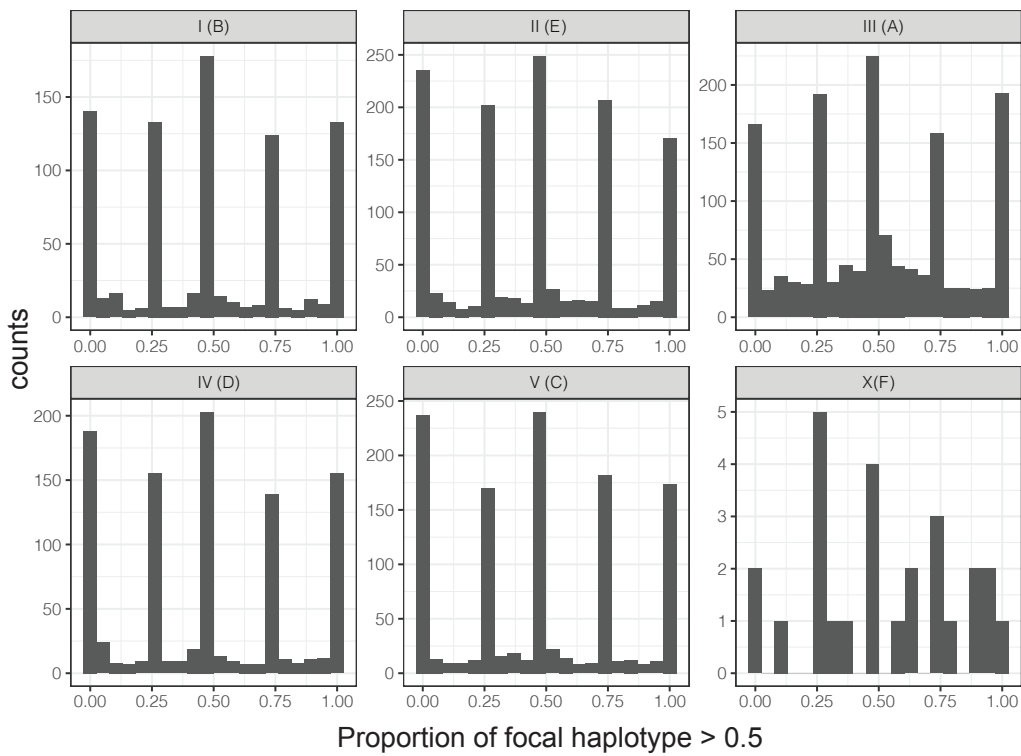
681

682

## Supplementary Materials

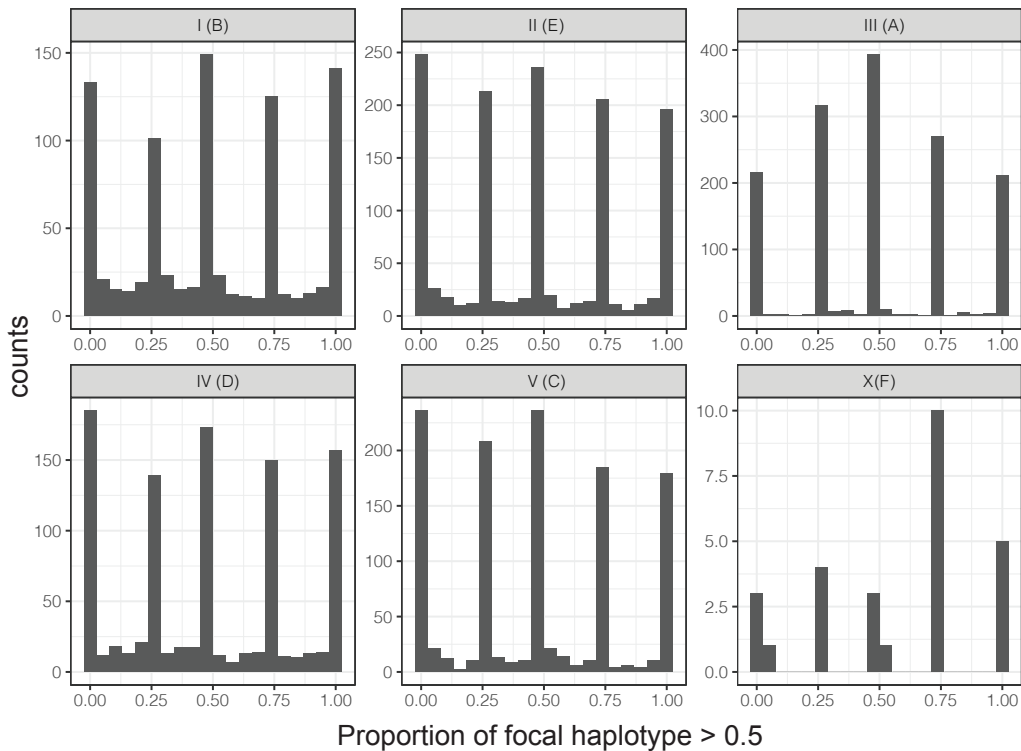
(A)

Genotypic (III<sup>M</sup>) males



(B)

Sex-reversed males



683

684 Supplementary Figure 1. Histograms of allele-specific expression (ASE) in genes for all  
685 chromosome are shown in the genotypic ( $III^M/III$ ) males and the sex-reversed ( $III/III$ ) males.  
686 Muller element nomenclature (from *Drosophila*) for each chromosome is given in parentheses. If  
687 a gene is expressed equally between two alleles, the proportion of focal haplotype is 0.5;  
688 otherwise, the proportion is greater or less than 0.5.



689 Supplementary Table 1. Chromosomal distribution of allele-specific expression (ASE) and no  
 690 allele-specific expression (non-ASE) in genotypic (III<sup>M</sup>) males and sex-reversed (SR) males.

Chromosome (Muller element)	# genes with ASE in III <sup>M</sup> males	# genes with non-ASE in III <sup>M</sup> males	# genes with ASE in SR males	# genes with non-ASE in SR males	Odds ratio	95% CI of odds ratio
III(A)	456	413	438	412	1.038574	0.8555646 - 1.2606663
<b>genome except III(A)</b>	<b>1635</b>	<b>1089</b>	<b>1711</b>	<b>1010</b>	<b>0.886281</b>	<b>0.7933539</b> - <b>0.9900421</b>
I(B)	320	222	334	212	0.915002	0.7123784 - 1.1750187
II(E)	465	314	513	291	0.840134	0.6821523 - 1.0344483
IV(D)	394	249	395	215	0.861373	0.6798614 - 1.0908786
V(C)	448	296	460	288	0.947652	0.7654588 - 1.1730543
X(F)	8	8	9	4	0.720539	0.102255 - 4.754933

691

692 Supplementary Table 2. Counts of genes with ASE on each chromosome in genotypic (III<sup>M</sup>)  
 693 males and sex-reversed (SR) males. The total number of genes (# genes) in each chromosome  
 694 group (second column), # genes with ASE in genotypic males and no ASE in sex-reversed males  
 695 (third column), and # genes with no ASE in genotypic males and ASE in sex-reversed males  
 696 (fourth column) are shown. Bold indicates statistical significance ( $P < 0.05$ )

		ASE in III <sup>M</sup> males and non-ASE in SR males	non-ASE in III <sup>M</sup> males and ASE in SR males	Fisher's Exact Test	
Chromosome (Muller element)	# genes	# genes	# genes	Odds ratio compared with III(A)	95% CI
III(A)	1420	95	76		
genome except III(A)	4201	<b>241</b>	<b>281</b>	<b>1.45665</b>	<b>1.014895 - 2.095777</b>
I(B)	824	51	59	1.444139	0.8688985 - 2.4078676
II(E)	1236	<b>68</b>	<b>86</b>	<b>1.578592</b>	<b>0.9961489 - 2.5100267</b>
IV(D)	966	<b>55</b>	<b>76</b>	<b>1.724145</b>	<b>1.063163 - 2.809137</b>
V(C)	1149	67	77	1.434875	0.8982881 - 2.2981210
X(F)	26	0	0	0	0 - Infinity

697

698 Supplementary Table 3. Counts of genes with allele-specific expression (ASE) based on division  
 699 of ASE measurements into five sections, following the rules described in the Methods. ASE  
 700 proportions are sorted in the order of extreme (1<sup>st</sup> and 5<sup>th</sup>), moderate (2<sup>nd</sup> and 4<sup>th</sup>), and no (3<sup>rd</sup>)  
 701 ASE. Only extreme ASE was used in the comparisons with no ASE.

Chr (ME)	Sections for ASE proportions	# of genes in genotypic (III <sup>M</sup> /III) Males			# of genes in sex-reversed (III/III) Males		
I (B)	1 <sup>st</sup> (extreme ASE)	167	320	627	167	334	667
	5 <sup>th</sup> (extreme ASE)	153			167		
	2 <sup>nd</sup> (moderate ASE)	158	307		167	333	
	4 <sup>th</sup> (moderate ASE)	149			166		
	3 <sup>rd</sup> (no ASE)	222	222		222	212	
II (E)	1 <sup>st</sup> (extreme ASE)	270	465	972	291	513	1013
	5 <sup>th</sup> (extreme ASE)	195			222		
	2 <sup>nd</sup> (moderate ASE)	251	507		258	500	
	4 <sup>th</sup> (moderate ASE)	256			242		
	3 <sup>rd</sup> (no ASE)	314	314		314	291	
III (A)	1 <sup>st</sup> (extreme ASE)	215	456	1043	220	438	1050
	5 <sup>th</sup> (extreme ASE)	241			218		
	2 <sup>nd</sup> (moderate ASE)	312	587		333	612	
	4 <sup>th</sup> (moderate ASE)	275			279		
	3 <sup>rd</sup> (no ASE)	413	413		413	412	
IV (D)	1 <sup>st</sup> (extreme ASE)	217	394	754	214	395	794
	5 <sup>th</sup> (extreme ASE)	177			181		
	2 <sup>nd</sup> (moderate ASE)	189	360		201	399	
	4 <sup>th</sup> (moderate ASE)	171			198		
	3 <sup>rd</sup> (no ASE)	249	249		249	215	
V (C)	1 <sup>st</sup> (extreme ASE)	258	448	891	268	460	908
	5 <sup>th</sup> (extreme ASE)	190			192		
	2 <sup>nd</sup> (moderate ASE)	220	443		239	448	
	4 <sup>th</sup> (moderate ASE)	223			209		
	3 <sup>rd</sup> (no ASE)	296	296		296	288	
X(F)	1 <sup>st</sup> (extreme ASE)	3	8	21	4	9	23
	5 <sup>th</sup> (extreme ASE)	5			5		
	2 <sup>nd</sup> (moderate ASE)	7	13		4	14	
	4 <sup>th</sup> (moderate ASE)	6			10		
	3 <sup>rd</sup> (no ASE)	5	5		5	4	

702  
 703  
 704  
 705  
 706  
 707  
 708

Supplementary Data 1. A VCF file called with the RNA-seq reads  
 Supplementary Data 2. A VCF file called with the Oxford Nanopore reads  
 Supplementary Data 3. IDP-ASE (allele-specific expression) output for the genotypic males  
 Supplementary Data 4. IDP-ASE (allele-specific expression) output for the sex-reversed males